Neurointerface implemented with Oscillator Motifs

Max Talanov[1,2], Alina Suleimanova[1,2], Alexey Leukhin[1,2], Yulia Mikhailova[1,2], Alexander Toschev[1,2], Alena Militskova[3], Igor Lavrov[1,5], Evgeni Magid[4]

***Abstract*— In this work, we present a definition of a neurointerface architecture combined from two main parts (1) neuroport (a hardware device) that implements a neuro protocol, generated and managed by a (2) neuroterminal (a software). The proposed architecture was created by analogy with OSI network architecture. We also present the neuroterminal as an oscillator motif real-time neurosimulation and results of the comparison of a bio-plausible motor pattern generated by oscillator motifs with square pulses of $20-40\,\mathrm{Hz}$ used as the neuro protocol for the output neuroport and measured their discomfort rate and efficacy according to an angle of subject fingers deflection. We determined that the most effective is the five oscillator motifs generated pattern for a median nerve stimulation, whereas for a muscle simulation $20\,\mathrm{a}$nd $40\,\mathrm{Hz}$ are more effective. We indicate that the oscillator motif generated pattern feels more natural than square pulses $20-40\,\mathrm{Hz}$, which feel like a spasm.**

I. Introduction

There are already exist a lot of promising projects in the field of brain-computer interface (BCI). Miguel Nicolelis [1], [2] controlled a robotic hand with a neuronal activity from a motor cortex of a monkey. Donoghue, Schwartz and Andersen [3], [4] reproduced control over a robotic arm via neuronal readouts using the three-dimensional tracking in virtual reality. Lebedev group [5] demonstrated the self-organisation of neural circuits of a brain to create the representation of robotic limbs in addition to biological limbs. The team of the Braingate project [6] demonstrated the brain implant to control a robotic arm by the neuronal activity, to move a subject's hand as well as a computer cursor, managing lights and TV. The commercial company Neuralink successfully presented a 1536-channel recording system for reading a brain activity [7] to control further neuroprosthesis. These projects are focused on an inbound brain-to-computer interface for readouts from a nervous system into a computing system.

As an example of digital devices to the nervous system interface and integration, it is worth mentioning the William Dobelle restore vision project [8]. The human brain project (HBP) [9] and Blue brain projects [10] are two huge European projects dedicated to a simulation of a partial or complete mammalian brain simulation. We indicate an important role of neurosimulation models that could be used as the part of a robotic system [11], or as a part of real time closed loop system for example projects simulating the spinal cord and nociceptive fibers [12], [13], [14].

There are several projects [15], [16], [17], [18] for the neurorehabilitation targeted to the motor control of subject limbs implemented as programmed neurostimulators demonstrated recently success. As examples of closed loop systems we should mention a number of interesting projects focused on Brain-Machine-Brain Interface [19], [20], [21], [22]

As the example of the brain network project, Pais-Vieira et al. [23] have connected several rat brains to a network of brains called Brainet. Yoo et al. integrated a human's brain with a spinal cord of a rat [24] controlling a locomotion of a rat tail.

Extending the presented above projects and concepts we introduce a high level approach for the inbound and outbound neurointerfaces combined from neuroterminal and neuroport described in details below. These concepts are concentrated around the neurosimulation as spiking neural network (SNN) and neuroterminal that were not done previously. The integration of the neurosimulation with biological muscles is novel in the context of BCI or AI.

II. Neurointerface architecture

We propose to use the following definitions to describe the neurointerface architecture.

Neurointerface (NI) is the generic term to identify a in- and outbound hardware/software for reading from a nervous system (filtering, spike sorting, etc) or digital input that could be used as an input from a nervous system, communication and writing into a nervous system (generating spike patterns, managing pulses, and their series, etc). Usually it is the part of a closed loop system (Fig. 1).

Neuroport (NP) is the part of NI, typically a hardware device that implements the neural interface protocol and runs the neuroterminal program. NP uses the analogy of the physical layer of the OSI model [25].

Neurointerface protocol (NIP) is a sequence of stimulus pulses (spikes) to activate a part of the nervous system with maximum efficiency and minimal discomfort for a subject.

Neuroterminal (NT) is the software/hardware system that implements the NIP with self-adaptation to a subject. It is usually a part of a closed-loop system that includes an NI. NT exploits the analogy with data link and network layers of the OSI model [25].

[1] B-Rain Labs LLC, Kazan, Russian Federation
[2] Neuromorphic computing and Neurosimulations laboratory, ITIS, Kazan Federal University, Russian Federation
[3] Institute of Fundamental Medicine and Biology, Kazan Federal University, Russian Federation
[4] Intelligent Robotic Systems Laboratory (LIRS), ITIS, Kazan Federal University, Russian Federation
[5] Department of Neurologic Surgery, Department of Physiology and Biomedical Engineering, Department of Neurology at Mayo Clinic, USA
Corresponding author: Max Talanov (max.talanov@gmail.com)

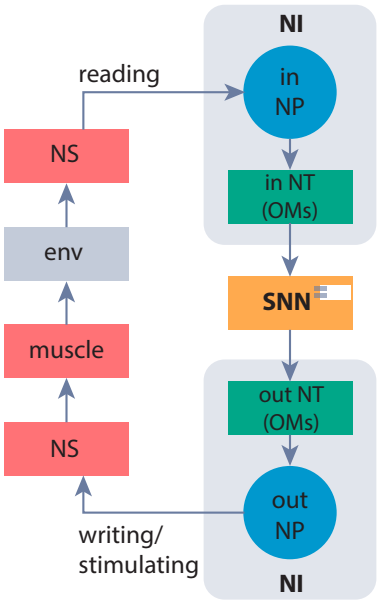

Fig. 1. Closed loop system with neurointerface identified. Blue is the physical, green – data link and network and orange – application layers; red – biological systems, gray – environment. Env stands for environment, NS – nervous system, NI – neurointerface, NP – neuroport, NT – neuroterminal, SNN – spiking neural network.

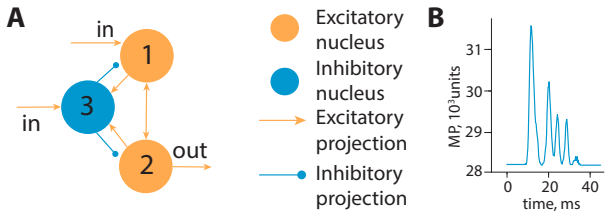

Fig. 2. Oscillator motif. Orange – excitatory, blue – inhibitory nuclei. **(A)** The oscillator motif circuit consist of three nuclei where 1st and 3rd receive input signal and 2nd transmits output neuronal activity. The 1st and 2nd nuclei form reciprocal excitation whereas these nuclei with 3rd nucleus organise the feed-back inhibition connection. **(B)** The output of one OM triggered by one stimulus.

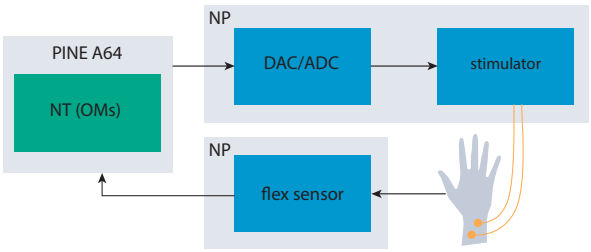

Fig. 3. The high-level design of the study to test the *out NI*. Blue – physical, green – data link and network layers. The NT is implemented in PINE A64 computer as the neural circuit of OMs. The generated neuronal activity is transmitted to the stimulator via DAC/ADC. The electrodes are located on the median nerve. The flex sensor is attached to the most indicative finger to estimate displacement.

The proposed neurointerface architecture is presented in Fig. 1 the main idea is a pipeline with the *input NP* and the *NT* being parts of the *in NI*. The *in NP* component could be some reading neuronal activity device like the patch clamp, voltage clamp, electrode arrays, myogram invasive/noninvasive electrodes, etc, as well as digital input devices like pressure, joint angle sensors, and controllers that transmit to an NT software/hardware. The *in NT* block could implement inbound signals prepossessing including filtering, spike sorting, spike time encoding and later transmission to an SNN. In case of digital input it could be implemented as spike times encoder hardware or software. The *SNN* component is simulation software/hardware of a part of a nervous system or the other software that could simulate a function of a part of nervous system (NS), for example navigation. The *out NT* is the software/hardware that processes the output (generated by the SNN) encoding it into sequence of low-level spiking patterns for the NS/muscles control. The *out NP* is the stimulation hardware implant or noninvasive stimulator for the NS or muscle stimulation. In the case of digital output this could be the hardware port for actuators, for example, locomotion controller. The *out NS* could be a part of the nervous system that is stimulated or activated whereas a muscle is a biological muscle or a digital hardware actuator as a part of a robotic system or an exoskeleton.

The main building block of the *out NT* is the oscillator motif (OM) circuit that includes two functional components as reciprocal excitation and feed-back inhibition (Fig. 2A) [26], [27]. It produces a neuronal activity with different duration, that depends on a weight balance between excitatory and inhibitory projections to and from the third nucleus (Fig. 2A) [28]. The first and second excitatory nuclei have a high weight (1850 and 1500 respectively) of reciprocal excitation projections to produce high-frequency output neuronal activity that is limited by the inhibitory projection from the third nucleus (negative weight -900), which has a relatively low (450) weight of projections from excitatory nuclei. Also, an external stimulus through the connection with weight 900 to the third nucleus could terminate output activity (Fig. 2A).

We use a set of weights that provides an output potential with few peaks (2-4). The average output activity of the 2nd nucleus is shown in Fig. 2B. We use a simple model of neurons presented in our previous article [29] to achieve the real-time simulation. The *out NT* uses the OMs to generate the bio-plausible neuronal activity to manage natural limbs through the *out NP*. Below we present the experimental research results of the implementation and testing of the *out NI*.

III. Methods

Five healthy subjects participated in the current study (3 male and 2 female, mean: 29.7 ± 10.1 years). All participants gave an informed written consent to participate in the experiment, in accordance with the Declaration of Helsinki. The experimental setup of the *out NI* is presented in Fig. 3. A single-board computer (PINE A64) that plays the role of NT generates the neuronal activity according to the number of OMs. It has inbound connections from NP (a flex sensor) and outbound NP (DAC/ADC). This activity is transmitted via DAC/ADC E-502-P-EU-D to the stimulator

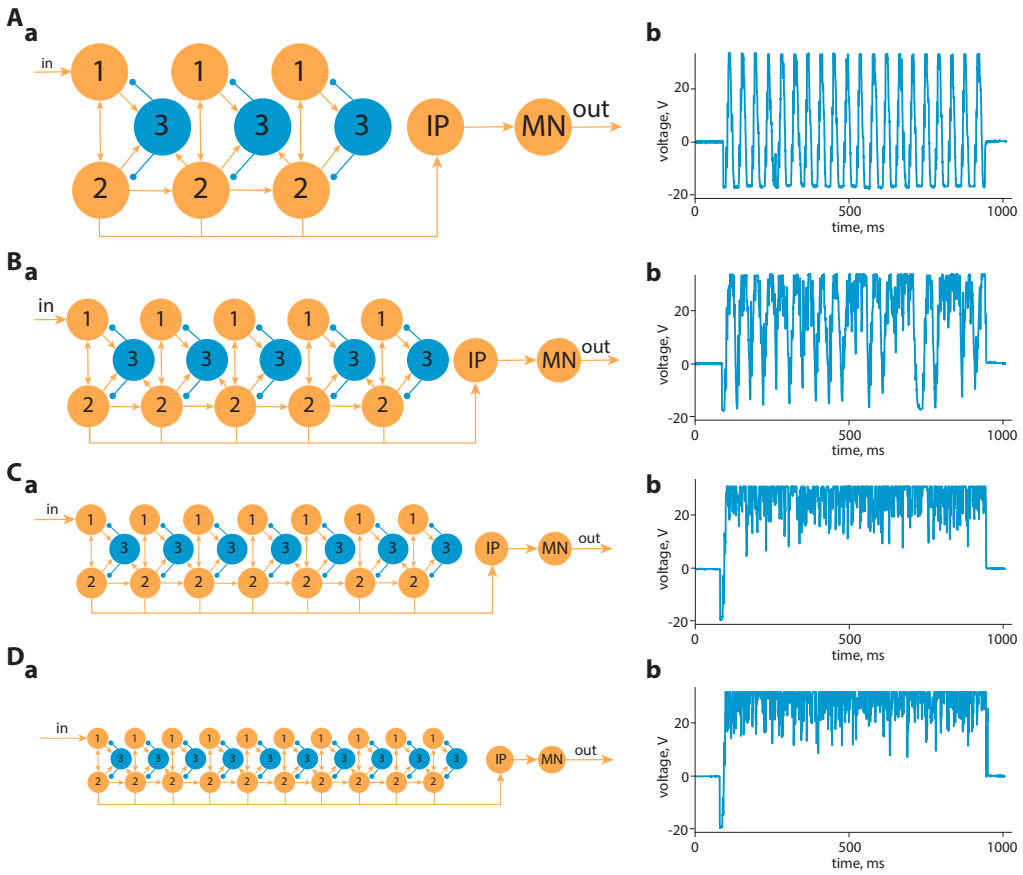

Fig. 4. The neural circuits based on **(Aa)** 3 OMs, **(Ba)** 5 OMs, **(Ca)** 7 OMs, **(Da)** 10 OMs that transmit neuronal activity to motoneurons (MN) via interneuronal pool (IP). The output neuronal activity of neural circuits based on **(Ab)** 3 OMs, **(Bb)** 5 OMs, **(Cb)** 7 OMs, **(Db)** 10 OMs.

(*out NP*) that innervates the median nerve to trigger a muscle. Non-invasive median nerve stimulation was performed with two hypoallergenic, reusable gel electrodes VUPIESSE $32\,\mathrm{mm} \times 32\,\mathrm{mm}$ for functional electrical stimulation, placed on the median nerve region of a right wrist or a finger flexor muscle (m. flexor digitorum superficialis), with a cathode being $2\,\mathrm{cm}$ proximal to an anode. The intensity of the electrical stimulation was adjusted to obtain a tingling sensation of a palm and a visible flexion response of an index and/or middle finger in each stimulation session and also kept to a comfortable range for a participant (up to the pain threshold). We attach the flex sensor FS-L-0112-103-ST (in NP) to a subject's hand by a velcro tape and calculated the displacement angle of the most indicative finger. The flex sensor was $112\,\mathrm{mm}$ long and has a linear resistance to angle function (the resistance with no bending is $15\,\mathrm{k}\Omega$). The resistance across the sensor increases as the sensor is being flexed in the range $60 - 110\,\mathrm{k}\Omega$ (resistance tolerance: $\pm 30\%$). The flex sensor was powered by $5\,\mathrm{V}$ from Pine A64 and had two $9.1\,\mathrm{k}\Omega$ series-connected resistors ($18.2\,\mathrm{k}\Omega$ total). The angle to voltage proportion for our setup is $1^\circ = 0.047\,\mathrm{V}$.

At the beginning of the experiment, we connected all parts as presented in Fig. 3 and set a number of OMs (out NT) or frequency of square pulses. We slightly increased the signal amplitude focusing on the participant's feelings. We registered the input neuronal activity going to the nerve (NS) at the output of the stimulator (out NP). We recorded flex sensor (in NP) output as the voltage between resistors. We made records with an oscilloscope, with each recording of 2 min long.

IV. Results

In this work we compared the effectiveness and the discomfort rate of the complex pattern generated by OMs and square pulses frequently used in muscle and neurostimulation [30].

In our experiments we varied teh number of OMs, schematics are presented in Fig. 4 Aa, Ba, Ca, Da, results are presented in Table I.

The first OM is triggered by the stimulus inbound to the 1st nucleus then it transmits the signal to next OM from the 2nd nucleus of the current OM to the 2nd nucleus of the following OM. The output neuronal activity from the 2nd nuclei of all OMs is transmitted to the interneuronal pool (IP) where it is integrated. The IP is connected with motoneurons (MN), their output neuronal activity is transmitted to the stimulator. Fig. 4 Ab, Bb, Cb, Db presents the results of simulation neuronal activity recorded by the digital oscilloscope Rigol DS1074Z.

The output neuronal activity was filled according to the

exp.	nerve stimulation			muscle stimulation		
	Threshold	Max	Angle	Threshold	Max	Angle
3 OM	51 ± 10.93	60.9 ± 6.71	44.4 ± 13.26	61 ± 3.24	65.4 ± 4.89	76.8 ± 31.11
5 OM	46.8 ± 12.64	58.8 ± 5.81	57.4 ± 32.16	57.2 ± 6.54	61.8 ± 8.76	69.1 ± 60.70
7 OM	47.6 ± 13.45	58.2 ± 7.05	44.9 ± 24.85	56.4 ± 6.54	61.3 ± 7.68	60.6 ± 32.84
10 OM	46 ± 10.56	56.4 ± 7.66	46.5 ± 30.28	52.9 ± 8.41	61.1 ± 7.50	53.8 ± 34.16
20Hz	30.6 ± 13.32	41.6 ± 13.94	28.6 ± 20.55	36.7 ± 6.46	48.7 ± 6.04	85.9 ± 20.82
40Hz	29.8 ± 3.21	38.3 ± 8.33	31.7 ± 17.39	35.2 ± 7.33	42.9 ± 7.39	86.5 ± 8.52
1kHz	34.3 ± 3.4	47.8 ± 8.77	58.2 ± 32.13	31.4 ± 2.53	36.6 ± 4.89	72.4 ± 29.85
3kHz	36.3 ± 8.38	49.3 ± 9.64	52.4 ± 31.95	33.7 ± 6.83	41.6 ± 8.44	79.3 ± 24.31
5kHz	39 ± 8.52	54.3 ± 10.44	70.3 ± 11.48	41.9 ± 9.62	43.1 ± 8.86	79.5 ± 33.14
7kHz	37.3 ± 3.4	56.3 ± 12.2	66.2 ±10.95	36.1 ± 8.63	50.2 ± 8.19	73.9 ± 27.66

TABLE I

EXPERIMENTAL RESULTS FOR DIFFERENT OM NUMBERS. THRESHOLD AND MAXIMUM IN V WHERE THE GREEN COLOUR HIGHLIGHTS MAX VOLTAGE AND THE RED COLOUR HIGHLIGHTS MIN VOLTAGE. FOR EFFECTIVENESS OF FINGER DISPLACEMENT IN DEGREES(°) THE GREEN COLOUR HIGHLIGHTS MAX ANGLE AND THE RED COLOUR HIGHLIGHTS MIN ANGLE. THE DATA PRESENTED IN FORMAT MEAN±SD

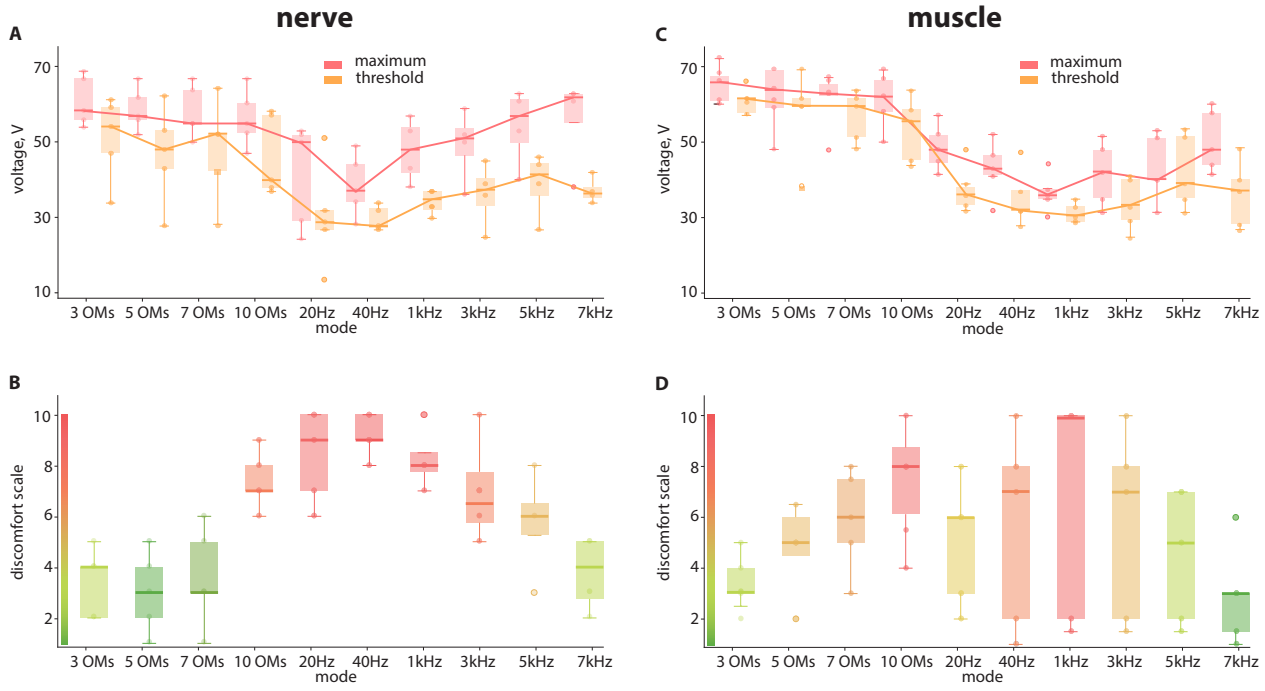

Fig. 5. **(A)** The distribution (n=5, number of subjects tested) of maximum discomfort voltage (red) and the threshold which was determined by flex sensor as the beginning of a movement (yellow) with nerve stimulation. **(B)** The distribution (n=5) of discomfort rate from 1 to 10 for different modes with nerve stimulation. **(C)** The distribution (n=5) of maximum discomfort voltage (red) and threshold (yellow) with muscle stimulation. **(D)** The distribution (n=6) of discomfort rate from 1 to 10 for different modes with muscle stimulation.

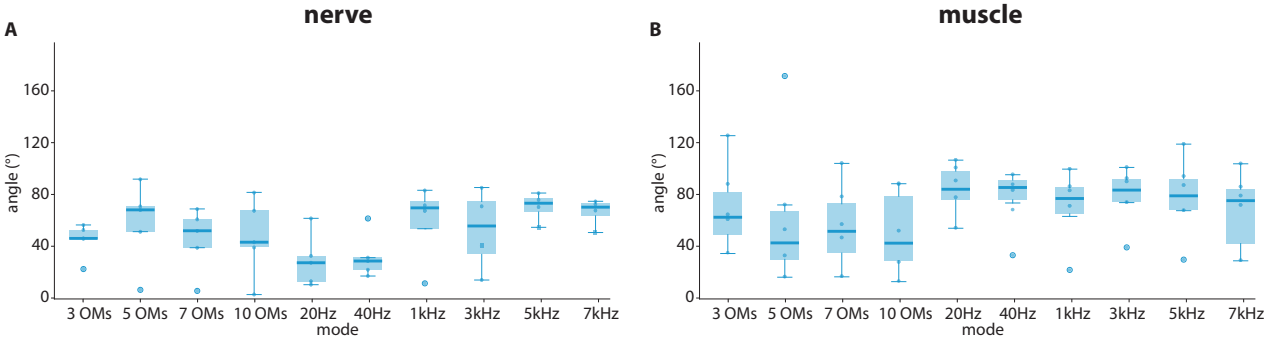

Fig. 6. **(A)** The distribution (n=5) of the finger displacement angle with nerve stimulation. **(B)** The distribution (n=5) of the finger displacement angle with muscle stimulation.

OMs number. There are the gaps between grouped neuronal activity with 3 and 5 OMs (Fig. 4 Ab, Bb), whereas 7 and 10 OMs output activity is almost continuous (Fig. 4 Cb, Db). The output neuronal activity from 3 and 5 OMs was shorter than a 50 ms window between 20 Hz pulses. The duration of neuronal activity triggered by one stimulus was 26 ms for 3 OMs, 43 ms for 5 OMs, 60 ms for 7 OMs, and 87 ms for 10 OMs. Therefore, in the case of 7 and 10 OMs, activity is overlapped and uninterrupted.

These differences influenced the sensation that were produced by the stimulation: the maximum discomfort voltage, the threshold, and the discomfort rate (Fig. 5). The discomfort rate was subjectively estimated by the participant's feelings in a scale from 1 (most comfort) to 10 (most discomfort).

We conducted experiments triggering the median nerve or finger flexor muscle. The most comfortable mode for the nerve stimulation was the 5 OMs (3.0/10, Fig. 5B). In addition, the maximum angle of finger displacement (57.4°) is shown (Fig. 6A) in this mode. The mode with 3 OMs has a slightly higher discomfort rate (3.4/10, Fig. 5B) but the angle of the finger deflection was lower (44.4°). The sensor threshold value is higher (51.6 V, Fig. 5A) than in mode with 5 OMs (46.8 V). The mode with 3 OMs is one of the most comfortable for the muscle stimulation (3.4/10, Fig. 5D) and also shows high angles of the finger displacement (76.8°).

In addition, we conducted experiments with 7 and 10 OMs that produced continuous neuronal activity without gaps (Fig. 4Cb, Db). The 7 OMs neuronal activity showed the 44.9° angle (Fig. 6A) and the low rate of discomfort (3.6/10) for the nerve stimulation whereas for the muscle stimulation we registered the higher angle (60.6°, Fig. 6B) and the discomfort scale 5.9/10. The maximum discomfort voltage and the threshold are close in case of the 5 OMs (Fig. 5A). The mode with 10 OMs has the lowest threshold and the maximum discomfort value (AVG 46 V and 56.4 V) and the highest discomfort rate (7.4 for the nerve and 6.7 for the muscle stimulation) between all modes with OMs, but with these parameters, the deflection angle was lower (46.5° for nerve and 53.8° for muscle stimulation, Fig. 6). Thus, the optimal modes for sensation and deflection angle are with 5 and 7 OMs for nerve stimulation and mode with 3 OMs for muscle stimulation.

The complex neuronal activity generated by the circuit of OMs shows satisfactory results both in sensations and in the finger movement amplitude. We compared the complex neuronal activity with square pulses to estimate effectiveness and discomfort rate. We used square pulses of 20 Hz and 40 Hz that are balanced around 0 V. With this kind of pulses, the maximum values and threshold were lower for both nerve and muscle stimulation (Fig. 5A, C), but the discomfort rates were different (Fig. 5B,D).

The angle was lower (28.6° for 20 Hz and 31.7° for 40 Hz, Fig. 6A) for nerve stimulation, but higher for muscle stimulation (85.9° for 20 Hz and 86.5° for 40 Hz, Fig. 6B). Besides, the movement was not rhythmic, but a single spasm contraction. Thus, we consider pulses generated by OMs more optimal than square pulses in terms of comfort and the finger displacement angle.

We also conducted experiments with high frequencies (kHz) to compare the sensations. The modes with 1 kHz and 3 kHz showed the low sensor threshold (Fig. 5A, C) and fairly high angles (Fig. 6A,B) for both the nerve and the muscle stimulation, however, the discomfort rates were high 8.25 for 1 kHz and 7 for 3 kHz for the nerve stimulation and slightly lower for the muscle stimulation (6.7 and 5.7). The highest angle of the finger displacement of kHz pulses was shown in mode with 5 kHz: 70.3° for the nerve and 79.5° for the muscle stimulation (Fig. 6A,B). The most comfortable mode of kHz pulses was 7 kHz (3.8 and 2.9, Fig. 5B,D), the angle was also high 66.2° for the nerve stimulation and 73.9° for the muscle stimulation. Thus, kHz pulses have shown good results we consider a possible modulation of neuronal OMs activity with a frequency of 7 kHz–10 kHz.

V. Conclusion

We proposed the high-level architecture of a bidirectional neurointerface consisting of the neuroport (NP) and the neuroterminal (NT). One of the options to create an *out NT* is to use the combination of oscillator motifs to generate a neuronal pattern used as the neurointerface protocol (NIP). We conducted experiments to determine the level of discomfort rate and the effectiveness measured as finger displacement angle of the stimulation impact. We compared the stimulation with the pattern generated by OMs form 3 to 10 in with square pulses 20 Hz and 40 Hz the most popular neurostimulation of a human spinal cord frequencies. For the median nerve stimulation square pulses used as neurointerface protocol indicated less effectiveness than patterns generated by OMs (Fig. 6A, 28.6° for 20 Hz and 31.7° for 40 Hz). In case of the muscle stimulation we indicate the higher effectiveness of 20 Hz and 40 Hz than OM generated patterns (Fig. 6B, 85.9° for 20 Hz and 86.5° for 40 Hz).

The discomfort rate of the 20 Hz and 40 Hz indicated highest values of the median nerve stimulation and median for the muscle stimulation (Fig. 5B,D). The 40 Hz muscle stimulation shows highest variability depending on the subjective feelings of participants based on their psychological and physiological states. We are planning to include more participants to obtain statistically significant data. We conducted series of experiments to identify the most comfortable modulation frequency of 7 kHz (Fig. 5B,D, AVG: 2.9/10 for the muscle and 3.75/10 for the nerve stimulation).

The nature of a muscle contraction is different in the case of square pulses, it feels like a spasm and in the case of a pattern, it feels like a directional muscle contraction with the frequency of the pattern. As a part of our ongoing research, we compare modulated patterns according to the effectiveness and the discomfort rate.

Acknowledgment

The authors would like to thank the B-Rain Labs LLC company for supporting their work with neurosimulations. The eighth author acknowledges the support of the Russian

Foundation for Basic Research (RFBR), project ID 19-58-70002. This work is the part of Kazan Federal University Strategic Academic Leadership Program.

REFERENCES

[1] J. Wessberg, C. R. Stambaugh, J. D. Kralik, P. D. Beck, M. Laubach, J. K. Chapin, J. Kim, S. J. Biggs, M. A. Srinivasan, and M. A. L. Nicolelis, "Real-time prediction of hand trajectory by ensembles of cortical neurons in primates," *Nature*, vol. 408, no. 6810, pp. 361–365, Nov. 2000, number: 6810 Publisher: Nature Publishing Group. [Online]. Available: https://www.nature.com/articles/35042582

[2] J. E. O'Doherty, M. A. Lebedev, P. J. Ifft, K. Z. Zhuang, S. Shokur, H. Bleuler, and M. A. L. Nicolelis, "Active tactile exploration using a brain–machine–brain interface," *Nature*, vol. 479, no. 7372, pp. 228–231, Nov. 2011, number: 7372 Publisher: Nature Publishing Group. [Online]. Available: https://www.nature.com/articles/nature10489

[3] M. Velliste, S. Perel, M. C. Spalding, A. S. Whitford, and A. B. Schwartz, "Cortical control of a prosthetic arm for self-feeding," *Nature*, vol. 453, no. 7198, pp. 1098–1101, Jun. 2008, number: 7198 Publisher: Nature Publishing Group. [Online]. Available: https://www.nature.com/articles/nature06996

[4] D. M. Taylor, S. I. H. Tillery, and A. B. Schwartz, "Direct Cortical Control of 3D Neuroprosthetic Devices," *Science*, vol. 296, no. 5574, pp. 1829–1832, Jun. 2002, publisher: American Association for the Advancement of Science Section: Research Article. [Online]. Available: https://science.sciencemag.org/content/296/5574/1829

[5] M. A. Lebedev and M. A. Nicolelis, "Brain-machine interfaces: From basic science to neuroprostheses and neurorehabilitation," *Physiological reviews*, vol. 97, no. 2, pp. 767–837, 2017.

[6] L. R. Hochberg, D. Bacher, B. Jarosiewicz, N. Y. Masse, J. D. Simeral, J. Vogel, S. Haddadin, J. Liu, S. S. Cash, P. van der Smagt, and J. P. Donoghue, "Reach and grasp by people with tetraplegia using a neurally controlled robotic arm," *Nature*, vol. 485, no. 7398, pp. 372–375, May 2012. [Online]. Available: https://www.ncbi.nlm.nih.gov/pmc/articles/PMC3640850/

[7] E. Musk and Neuralink, "An integrated brain-machine interface platform with thousands of channels," Neuroscience, preprint, Jul. 2019.

[8] S. Kotler, "Vision Quest," accessed: 2021-02-02. [Online]. Available: www.wired.com/2002/09/vision/

[9] H. Markram, K. Meier, T. Lippert, S. Grillner, R. Frackowiak, S. Dehaene, A. Knoll, H. Sompolinsky, K. Verstreken, J. DeFelipe *et al.*, "Introducing the human brain project," *Procedia Computer Science*, vol. 7, pp. 39–42, 2011.

[10] H. Markram, "The blue brain project," *Nature Reviews Neuroscience*, vol. 7, no. 2, pp. 153–160, 2006.

[11] E. Chebotareva, R. Safin, A. Shafikov, D. Masaev, A. Shaposhnikov, I. Shayakhmetov, E. Magid, N. Zilberman, Y. Gerasimov, and M. Talanov, "Emotional Social Robot "Emotico"," in *2019 12th International Conference on Developments in eSystems Engineering (DeSE)*. Kazan, Russia: IEEE, Oct. 2019, pp. 247–252.

[12] M. Capogrosso, N. Wenger, S. Raspopovic, P. Musienko, J. Beauparlant, L. Bassi Luciani, G. Courtine, and S. Micera, "A Computational Model for Epidural Electrical Stimulation of Spinal Sensorimotor Circuits," *Journal of Neuroscience*, vol. 33, no. 49, pp. 19 326–19 340, Dec. 2013. [Online]. Available: http://www.jneurosci.org/cgi/doi/10.1523/JNEUROSCI.1688-13.2013

[13] I. A. Rybak, K. J. Dougherty, and N. A. Shevtsova, "Organization of the mammalian locomotor cpg: review of computational model and circuit architectures based on genetically identified spinal interneurons," *eNeuro*, vol. 2, no. 5, 2015.

[14] A. Suleimanova, M. Talanov, O. Gafurov, F. Gafarov, K. Koroleva, A. Virenque, F. M. Noe, N. Mikhailov, A. Nistri, and R. Giniatullin, "Modeling a Nociceptive Neuro-Immune Synapse Activated by ATP and 5-HT in Meninges: Novel Clues on Transduction of Chemical Signals Into Persistent or Rhythmic Neuronal Firing," *Frontiers in Cellular Neuroscience*, vol. 14, 2020, publisher: Frontiers. [Online]. Available: https://www.frontiersin.org/articles/10.3389/fncel.2020.00135/full

[15] F. B. Wagner, J.-B. Mignardot, C. G. L. Goff-Mignardot, R. Demesmaeker, S. Komi, M. Capogrosso, A. Rowald, I. Seáñez, M. Caban, E. Pirondini, M. Vat, L. A. McCracken, R. Heimgartner, I. Fodor, A. Watrin, P. Seguin, E. Paoles, K. V. D. Keybus, G. Eberle, B. Schurch, E. Pralong, F. Becce, J. Prior, N. Buse, R. Buschman, E. Neufeld, N. Kuster, S. Carda, J. v. Zitzewitz, V. Delattre, T. Denison, H. Lambert, K. Minassian, J. Bloch, and G. Courtine, "Targeted neurotechnology restores walking in humans with spinal cord injury," *Nature*, vol. 563, no. 7729, p. 65, Nov. 2018.

[16] M. L. Gill, P. J. Grahn, J. S. Calvert, M. B. Linde, I. A. Lavrov, J. A. Strommen, L. A. Beck, D. G. Sayenko, M. G. V. Straaten, D. I. Drubach, D. D. Veith, A. R. Thoreson, C. Lopez, Y. P. Gerasimenko, V. R. Edgerton, K. H. Lee, and K. D. Zhao, "Neuromodulation of lumbosacral spinal networks enables independent stepping after complete paraplegia," *Nature Medicine*, 2018.

[17] R. C. Venancio, S. Pelegrini, D. Q. Gomes, E. Y. Nakano, and R. E. Liebano, "Effects of Carrier Frequency of Interferential Current on Pressure Pain Threshold and Sensory Comfort in Humans," *Archives of Physical Medicine and Rehabilitation*, vol. 94, no. 1, pp. 95–102, Jan. 2013.

[18] X. Bao, Y. Zhou, Y. Wang, J. Zhang, X. Lü, and Z. Wang, "Electrode placement on the forearm for selective stimulation of finger extension/flexion," *PLOS ONE*, vol. 13, no. 1, p. e0190936, Jan. 2018.

[19] S. J. Bensmaia and L. E. Miller, "Restoring sensorimotor function through intracortical interfaces: progress and looming challenges," *Nature Reviews Neuroscience*, vol. 15, no. 5, pp. 313–325, May 2014, number: 5 Publisher: Nature Publishing Group. [Online]. Available: https://www.nature.com/articles/nrn3724

[20] E. E. Fetz, "Chapter 12 - Restoring motor function with bidirectional neural interfaces," in *Progress in Brain Research*, ser. Sensorimotor Rehabilitation, N. Dancause, S. Nadeau, and S. Rossignol, Eds. Elsevier, Jan. 2015, vol. 218, pp. 241–252. [Online]. Available: http://www.sciencedirect.com/science/article/pii/S0079612315000023

[21] M. A. Lebedev, A. J. Tate, T. L. Hanson, Z. Li, J. E. O'Doherty, J. A. Winans, P. J. Ifft, K. Z. Zhuang, N. A. Fitzsimmons, D. A. Schwarz, A. M. Fuller, J. H. An, and M. A. L. Nicolelis, "Future developments in brain-machine interface research," *Clinics*, vol. 66, pp. 25–32, 2011, publisher: Faculdade de Medicina / USP. [Online]. Available: http://www.scielo.br/scielo.php?script=sci_abstract&pid=S1807-59322011001300004&lng=en&nrm=iso&tlng=en

[22] M. A. L. Nicolelis and M. A. Lebedev, "Principles of neural ensemble physiology underlying the operation of brain–machine interfaces," *Nature Reviews Neuroscience*, vol. 10, no. 7, pp. 530–540, Jul. 2009, number: 7 Publisher: Nature Publishing Group. [Online]. Available: https://www.nature.com/articles/nrn2653

[23] M. Pais-Vieira, G. Chiuffa, M. Lebedev, A. Yadav, and M. A. L. Nicolelis, "Building an organic computing device with multiple interconnected brains," *Scientific Reports*, vol. 5, no. 1, p. 11869, Jul. 2015, number: 1 Publisher: Nature Publishing Group. [Online]. Available: https://www.nature.com/articles/srep11869).

[24] S.-S. Yoo, H. Kim, E. Filandrianos, S. J. Taghados, and S. Park, "Non-Invasive Brain-to-Brain Interface (BBI): Establishing Functional Links between Two Brains," *PLOS ONE*, vol. 8, no. 4, p. e60410, Apr. 2013, publisher: Public Library of Science. [Online]. Available: https://journals.plos.org/plosone/article?id=10.1371/journal.pone.0060410

[25] D. Steedman, "Open systems interconnection protocols," in *Information Technology and the Computer Network*, K. G. Beauchamp, Ed. Berlin, Heidelberg: Springer Berlin Heidelberg, 1984, pp. 193–202.

[26] J. T. Paz and J. R. Huguenard, "Microcircuits and their interactions in epilepsy: is the focus out of focus?" *Nature Neuroscience*, vol. 18, no. 3, pp. 351–359, 2015.

[27] T. Womelsdorf, T. A. Valiante, N. T. Sahin, K. J. Miller, and P. Tiesinga, "Dynamic circuit motifs underlying rhythmic gain control, gating and integration," *Nature Neuroscience*, vol. 17, no. 8, pp. 1031–1039, Aug. 2014.

[28] M. Talanov, A. Leukhin, A. Suleimanova, A. Toschev, and I. Lavrov, "Oscillator Motif as Design Pattern for the Spinal Cord Circuitry Reconstruction," *BioNanoScience*, 2020. [Online]. Available: https://link.springer.com/epdf/10.1007/s12668-020-00743-z

[29] A. Leukhin, M. Talanov, A. Suleimanova, A. Toschev, and I. Lavrov, "Even simpler real-time model of neuron," *BioNanoScience*, pp. 1–4, 2020.

[30] M. Gill, M. Linde, K. Fautsch, R. Hale, C. Lopez, D. Veith, J. Calvert, L. Beck, K. Garlanger, R. Edgerton *et al.*, "Epidural electrical stimulation of the lumbosacral spinal cord improves trunk stability during seated reaching in two humans with severe thoracic spinal cord injury," *Frontiers in Systems Neuroscience*, vol. 14, 2020.